



**HAL**  
open science

# Modelling the optical turbulence boiling and its effect on finite-exposure differential image motion

A. Berdja, J. Borgnino

► **To cite this version:**

A. Berdja, J. Borgnino. Modelling the optical turbulence boiling and its effect on finite-exposure differential image motion. *Monthly Notices of the Royal Astronomical Society*, 2007, 378, pp.1177-1186. hal-00417113

**HAL Id: hal-00417113**

**<https://hal.science/hal-00417113>**

Submitted on 19 Nov 2021

**HAL** is a multi-disciplinary open access archive for the deposit and dissemination of scientific research documents, whether they are published or not. The documents may come from teaching and research institutions in France or abroad, or from public or private research centers.

L'archive ouverte pluridisciplinaire **HAL**, est destinée au dépôt et à la diffusion de documents scientifiques de niveau recherche, publiés ou non, émanant des établissements d'enseignement et de recherche français ou étrangers, des laboratoires publics ou privés.



Distributed under a Creative Commons Attribution 4.0 International License

# Modelling the optical turbulence boiling and its effect on finite-exposure differential image motion

A. Berdja<sup>1,2★</sup> and J. Borgnino<sup>2★</sup>

<sup>1</sup>*CRAAG, BP 63, Route de l'Observatoire, 16340 Bouzaréah, Alger, Algeria*

<sup>2</sup>*LUAN-UMR 6525, Université de Nice-Sophia Antipolis, Parc Valrose F-06108 Nice Cedex 2, France*

Accepted 2007 April 13. Received 2007 April 12; in original form 2006 October 11

## ABSTRACT

It is usually accepted that whenever dealing with astronomical observation through the atmosphere, the optical turbulence temporal evolution can be sufficiently described with the so-called frozen turbulence hypothesis. In this model, turbulence is supposed to be equivalent to a series of solid phase screens that slide horizontally in front of the observation field of view. Experimental evidence shows, however, that an additional physical process must be taken into account when describing the temporal behaviour of the optical turbulence. In fact, while translating above the observer, turbulence undergoes a proper temporal evolution and affects differently the astronomical and, more specifically, the astrometric observations. The proper temporal evolution of the turbulence-induced optical turbulence observable quantities is here called the optical turbulence boiling. We are proposing through this paper a theoretical approach to the modelling of the optical turbulence temporal evolution when the turbulent layer horizontal translation and the optical turbulence boiling are both involved. The model we propose, as a working hypothesis though, has a direct relevance to differential astrometry because of its explicit dependence upon the optical turbulence temporal evolution. It can also be generalized to other techniques of high angular resolution astronomical observation through the atmospheric turbulence.

**Key words:** turbulence – atmospheric effects – techniques: high angular resolution – astrometry – planetary systems.

## 1 INTRODUCTION

One of the most exciting astronomical activities nowadays is incontestably the detection of extra-solar planetary systems. For this purpose, and in parallel to direct imaging developments (Chauvin et al. 2005), many indirect observation methods are being developed. Astrometry, complementarily to radial velocity surveys, appears to be a promising technique for exoplanet detection through its capability to determine planetary masses and long-period orbits (McAlister 1996; Pravdo & Shaklan 1996; Launhardt 2005). The accuracies needed today for detecting the astrometric signature of the apparent star position perturbation that is induced by an orbiting planet in a nearby system are of the order of a few microarcseconds if not less (Sozzetti 2005). In order to detect these astrometric signatures, space and ground-based astrometric programmes are being developed (Casertano et al. 1996; Lattanzi et al. 2000; Sozzetti et al. 2003). The most straightforward direction for ground-based astrometry to achieve such precisions is probably related to infrared long-baseline interferometry (Shao & Colavita 1992; Lane & Mutterspaugh 2004).

It appears, however, that with appropriate field averaging and data reduction (Pravdo & Shaklan 1996), an appropriate apodization of the entrance pupil and a virtually enhanced symmetrization of the reference field (Lazorenko & Lazorenko 2004; Lazorenko 2006), it is still possible to achieve very acceptable astrometric accuracies with mono-aperture telescopes (Gatewood 1987; Anderson et al. 2006) in relatively good seeing conditions.

Ground-based astrometry, like the other optical and infrared high angular resolution observation techniques, is strongly contaminated by the atmospheric optical turbulence. A long-exposure observation regime is therefore performed in order to induce a time averaging of the apparent instantaneous turbulence-induced image motion over the telescope field of view. For a given exposure time, the astrometric accuracy depends mostly upon how fast the optical turbulence evolves over time (Lindgren 1980). We find it important therefore to accurately model the optical turbulence temporal evolution and its effect on finite-exposure image motion in order to have the ability to perform the astrometrical measurements in the most suitable conditions.

The optical turbulence temporal evolution is usually modelled with the so-called frozen turbulence hypothesis or the Taylor hypothesis (Tatarskii 1971; Conan, Rousset & Madec 1995; Avila

\*E-mail: berdja@unice.fr (AB); borgnino@unice.fr (JB)

et al. 1997). The optical turbulence horizontal transportation has been observed for a long time (Vernin & Roddier 1973) and a model of multilayered frozen and translating turbulent layers has been developed (Roddier, Gilli & Lund 1982) for the purpose of studying the turbulence-induced speckle image temporal evolution (Aime, Kadiri & Ricort 1980; Aime et al. 1986; Vernin et al. 1991) and how to monitor it (Lopez 1992). It is still in use also to model speckle statistics in adaptively corrected images (Fitzgerald & Graham 2006). This multilayered approach is usually called ‘speckle boiling’. This denomination is due to the visual effect it induces on the speckle image temporal evolution and has nothing to do with the optical turbulence boiling we are describing in this paper. The frozen turbulence hypothesis is based upon the belief that for short exposure times, wavefronts do not deform but translate uniformly as the wind blows. This is equivalent, relatively to the optical effect that is induced, to moving solid diffusers illuminated using laser beams. It leads to a relatively simple theoretical description of the optical turbulence temporal evolution and how it is decorrelated over time (Conan et al. 1995). However, a closer look via dedicated experiments (St-Jacques 1998; Schöck & Spillar 1999) has given a new insight into the limits of the frozen turbulence hypothesis. It appears that this approximation is valid only for exposures lower than a few tens of milliseconds (St-Jacques & Baldwin 2000; Schöck & Spillar 2000) and that the optical turbulence temporal evolution cannot be described only by wavefront horizontal translation as it is usually supposed. This limit was also noted before (Gendron & Léna 1996). In fact, while translating in front of the telescope field of view, the optical turbulence undergoes a proper temporal evolution, which for a stationary observer superposes on that evolution produced by the horizontal transportation. This proper temporal evolution is to be referred to as the optical turbulence boiling.

A more appropriate modelling of the properties of the optical turbulence temporal evolution not only is relevant for long exposures as in astrometric surveys but also matters in some other high angular resolution techniques. For example, optimizing the response of adaptive optical systems depends upon the short time-scale over which the turbulence-induced optical wavefront pattern evolves. The deterministic aspect of the horizontal frozen and translating turbulent layers might also allow making predictions on the evolution of the wavefront pattern and thus making adaptive optics more efficient. The optical turbulence temporal evolution is also significant for long-baseline interferometry (Kellerer & Tokovinin 2007). It appears then that the validity of the frozen turbulence hypothesis as well as the influence of the optical turbulence boiling deserves to be discussed.

The major aim of the present paper is to propose a theoretical approach that permits modelling the optical turbulence temporal evolution when the optical turbulence boiling and the turbulence layer horizontal translating are both involved. We emphasize modelling the finite-exposure differential image motion because of its significance for astrometry and for the other techniques of high angular resolution imaging. The model can be easily generalized to other observable quantities as well.

## 2 FINITE-EXPOSURE DIFFERENTIAL IMAGE MOTION

When propagating through the atmosphere, light from outer space encounters a medium with a randomly distributed and time-changing refractive index field. This inhomogeneity is due to the omnipresent turbulence in the air. The different areas of an incoming wavefront are unequally slowed down by the refraction index field

and thus undergo phase and amplitude fluctuations (Tatarskii 1971). When diffraction occurs at the entrance pupil of a telescope and light is focused on an imaging detector, the instantaneous point spread function, which is the image obtained when a single unresolved star is observed, usually exhibits a speckled distribution rather than a single airy spot. This image is also shifted from its real position and as time passes by, its instantaneous position fluctuates around its average turbulence-free position. We do not discuss here the systematic errors like the differential chromatic refraction (Gubler & Tytler 1998), but we focus on the optical turbulence effects only. Image motion is due to the turbulence-induced angular deviations of light from its initial direction of incidence. It is proportional to the normalized averaging of the local wavefront slopes over the entrance pupil where they are weighted by the instantaneous intensity fluctuations resulting from scintillation (Tatarskii 1971).

Let  $\alpha_1(t)$  and  $\alpha_2(t)$  be the one-dimensional components along an arbitrary direction of the instantaneous angular motion of the images of two stars 1 and 2. One of them may be the target star under investigation and the other may be any of the reference stars in the field of view. Instantaneous differential image motion along that same direction is given by the difference  $\alpha_1(t) - \alpha_2(t)$  of the instantaneous departures  $\alpha_1(t)$  and  $\alpha_2(t)$  from the real positions of the stars as they should be measured without optical turbulence.

In the following, mono-directional differential image motion refers to the one-dimensional component of the two-dimensional differential image motion along a given orientation. The astrometric error can be defined as the rms of the long-exposure two-dimensional differential image motion. It can be easily obtained, for example, from the statistical variance of long-exposure mono-directional differential image motion taken along two arbitrary orthogonal orientations. In the following, we will focus, however, on the statistics of the finite-exposure mono-directional differential image motion.

In order to minimize the differential image motion effect on the angular separation measurements, a long-exposure measurement is performed in order to induce sufficient averaging on the instantaneous turbulence-induced motions. Because time averaging is finite, there always remains a residual differential image motion (Lindgren 1980).

If  $\Delta\alpha_{\text{res}}(T)$  is the residual mono-directional differential image motion after an averaging over a finite-exposure time  $T$ , then we write

$$\Delta\alpha_{\text{res}}(T) = \frac{1}{T} \int_0^T dt [\alpha_1(t) - \alpha_2(t)], \quad (1)$$

where  $\Delta\alpha_{\text{res}}(T)$  is simply the finite-exposure measurement of the mono-directional differential image motion  $\alpha_1 - \alpha_2$  over an exposure time  $T$ . It is a random quantity with zero mean like  $\alpha_1(t)$  and  $\alpha_2(t)$ . We will characterize it by its statistical variance  $\sigma_T^2$  that is given by

$$\sigma_T^2 = \langle |\Delta\alpha_{\text{res}}(T)|^2 \rangle, \quad (2)$$

where  $\langle \dots \rangle$  denotes ensemble averaging as if finite-exposure measurements were repeated infinitely with the same conditions of optical turbulence.

The statistical variance of the finite-exposure differential image motion can therefore be developed into

$$\sigma_T^2 = \int_0^T \int_0^T \frac{dt dt'}{T^2} \langle [\alpha_1(t) - \alpha_2(t)][\alpha_1(t') - \alpha_2(t')] \rangle. \quad (3)$$

The quantity that appears in the double integral is the temporal covariance  $R_{\Delta\alpha}(t - t')$  of the instantaneous differential image motion. As it depends only upon the time difference  $\tau = t - t'$ , the

double integral can be reduced into a single integral relatively to the variable  $\tau$ . We have thus

$$\sigma_T^2 = \frac{2}{T^2} \int_0^T d\tau [T - \tau] R_{\Delta\alpha}(\tau). \quad (4)$$

We can already see in this expression that the astrometrical error via the residual mono-directional differential image motion variance depends upon the statistical properties of the temporal evolution of the optical turbulence, which is expressed here through the temporal covariance of the instantaneous mono-directional differential image motion.

The temporal covariance  $R_{\Delta\alpha}(\tau)$  is directly related by a Fourier transform to the temporal power spectral density  $\omega_{\Delta\alpha}(\nu)$  of the instantaneous mono-directional differential image motion where  $\nu$  denotes a temporal frequency. The temporal power spectral density is a positive and pair function so that one directly writes

$$R_{\Delta\alpha}(\tau) = 2 \int_0^\infty d\nu \omega_{\Delta\alpha}(\nu) \cos[2\pi\nu\tau]. \quad (5)$$

The variance of the finite-exposure mono-directional differential image motion is then obtained with

$$\sigma_T^2 = \frac{4}{T^2} \int_0^T d\tau [T - \tau] \int_0^\infty d\nu \omega_{\Delta\alpha}(\nu) \cos[2\pi\nu\tau]. \quad (6)$$

One has, thus, to determine the temporal power spectral density of the instantaneous differential image motion in order to characterize long-exposure measurements.

While the modelling of the temporal statistical properties of the optical turbulence quantities is based upon the temporal power spectral density, the optical turbulence properties are most often described by the two-dimensional spatial power spectral density. In all the following, we will describe the effects induced by a single equivalent turbulent layer at a given altitude. We will also ignore the polychromatic effects on mono-directional differential image motion statistics (Berdja, Borgnino & Irbah 2006) and consider just the monochromatic case. If the optical turbulence obeys the von K arm an (Borgnino 1990; Borgnino, Martin & Ziad 1992) and Hill-Andrews models (Innocenti & Consortini 2004; Jolissaint, V eran & Conan 2006), then the instantaneous differential image motion spatial power spectral density  $W_{\Delta\alpha}(f)$ , where  $f$  is a two-dimensional spatial frequency vector, is given by

$$\begin{aligned} W_{\Delta\alpha}(f) = & 0.7654 \left[ \frac{C_n^2 \delta h}{\cos\{\varepsilon\}} \right] f_x^2 [f^2 + L_0^{-2}]^{-11/6} \\ & \times \left[ \frac{2DJ_1\{\pi Df\} - 2D'J_1\{\pi D'f\}}{\pi[D^2 - D'^2]f} \right]^2 \cos^2\{\pi\lambda h f^2\} \\ & \times [1 + 3.4310fl_0 - 0.5384[fl_0]^{7/6}] \exp\{-3.6252[fl_0]^2\} \\ & \times [1 - \cos\{2\pi h f \Theta\}], \end{aligned} \quad (7)$$

with  $f = f_x i + f_y j$ .

$\Theta = \Theta_x i + \Theta_y j$  is the two-dimensional angular separation between the two stars in the sky (Fig. 1),  $C_n^2$  the constant structure for refractive index fluctuations,  $\delta h$  the turbulent layer thickness,  $\varepsilon$  the average zenith angle,  $L_0$  the outer scale of the optical turbulence (Borgnino 1990; Borgnino et al. 1992),  $l_0$  the inner scale (Innocenti & Consortini 2004),  $D$  the diameter of the circular entrance pupil of the telescope,  $D'$  the diameter of the circular central obstruction,  $\lambda$  the light wavelength and  $h$  the altitude of the turbulent layer above the instrument. We have assumed here that the one-dimensional component of the differential image motion is oriented along the  $x$ -axis. The geometrical configuration is summarized in Fig. 1.

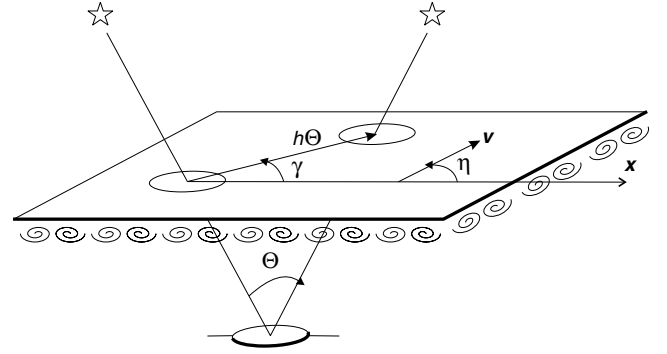


**Figure 1.** The plane surface in this diagram represents a horizontal turbulent layer at an altitude  $h$  above the ground-based telescope which is represented here by its entrance circular pupil downside. Two unresolved stars with angular separation  $\Theta$  are observed and the intersections of the lines of sight with the turbulent layer draw a baseline  $h\Theta$  which can be viewed as a projection of the angular separation. In the figure, the  $x$ -axis denotes the orientation along which the one-dimensional component of image motion is considered. The relative angle of the baseline to the image motion component is denoted by  $\gamma$ . The relative angle of the turbulence translation velocity  $v$  to the image motion component is denoted by  $\eta$ .

We should note here that one could obtain straightforward results for the long-exposure two-dimensional differential image motion from the following model just by replacing the term  $f_x^2$  by  $f^2$  in equation (7). Applications to some other optical turbulence observable quantities can be obtained by entering the appropriate spatial power spectral densities instead of the one expressed in the previous equation.

We will discuss in the following sections how to derive temporal power spectral densities from spatial power spectral densities in order to model the temporal statistical properties of the optical turbulence and their influence on high angular resolution techniques.

### 3 THE OPTICAL TURBULENCE TEMPORAL EVOLUTION PROCESSES

From the observational viewpoint, we can classify the optical turbulence temporal evolution according to two main phenomenological processes.

(i) A chaotic dynamical evolution, due to the very intrinsic nature of fluid turbulence, which causes what we have designated as the optical turbulence boiling. This process can be schematically described as being due to the fact that inside a turbulent layer, the relative spatial configuration of eddies at all available scales does change over time.

(ii) An apparent evolution that is due to the relative horizontal translation of the turbulent layer relatively to the observer. For a given line of sight, light experiences different parts of the turbulent layer over time.

We will first review the analytical modelling of the temporal power spectral density of the instantaneous mono-directional differential image motion when horizontal translation occurs alone without any proper boiling. This is the well-known frozen turbulence hypothesis. We present then an analytical modelling of the temporal power spectral density of the instantaneous mono-directional differential image motion when the optical turbulence boiling occurs alone. In the following section, we present a more general approach to model the temporal power spectral density of the

mono-directional instantaneous differential image motion when the turbulent layer horizontal translation and the optical turbulence boiling occur together.

#### 4 THE FROZEN TURBULENCE HYPOTHESIS

In this approximation, we consider that the optical turbulence temporal evolution is dominated by the translational effect as if the turbulence spatial pattern was frozen and entirely translated by the wind with a constant velocity  $\mathbf{v}$ . The frozen turbulence hypothesis is valid for a limited time beyond which we could consider that the optical turbulence boiling could become sufficiently important to induce additive temporal decorrelation.

Let  $\Delta\alpha(\mathbf{r}, t)$  be an instantaneous spatial distribution of the  $x$ -oriented mono-directional differential image motion as measured through a ground-based telescope, where  $\mathbf{r} = x\mathbf{i} + y\mathbf{j}$  is a two-dimensional position vector.

At an arbitrary initial instant  $t = 0$ , one can write

$$\Delta\alpha(\mathbf{r}, 0) = \int d\mathbf{f} |\overline{\Delta\alpha}(\mathbf{f}, 0)| \exp\{2\pi i \mathbf{f}\mathbf{r} + i\varphi_0(\mathbf{f})\}, \quad (8)$$

where  $|\overline{\Delta\alpha}(\mathbf{f}, 0)|$  is the modulus of the spatial Fourier transform of  $\Delta\alpha(\mathbf{r}, 0)$ . It is to be considered as a random quantity whose statistical variance gives the spatial power spectral density of the instantaneous differential image motion like the one given in equation (7).  $\varphi_0(\mathbf{f})$  is a random arbitrary phase with  $0 < \varphi_0(\mathbf{f}) \leq 2\pi$ . We might recall here that  $\Delta\alpha(\mathbf{r}, 0)$  is a random and unpredictable spatial distribution whose Fourier transform has random spatial frequency-distributed modulus  $|\overline{\Delta\alpha}(\mathbf{f}, 0)|$  and phase  $\varphi_0(\mathbf{f})$ . Only reproducible are the statistical quantities like the spatial power spectrum  $W_{\Delta\alpha}(\mathbf{f})$ , which is given by  $W_{\Delta\alpha}(\mathbf{f}) = \langle |\overline{\Delta\alpha}(\mathbf{f}, 0)|^2 \rangle$ .

During a finite duration  $t$ , the whole turbulence is translated along a distance  $\mathbf{v}t$  where  $\mathbf{v}$  is still the velocity vector of the turbulence translation. At an instant  $t$ , the observed optical turbulence pattern through a fixed line of sight at a position  $\mathbf{r}$  is the same pattern that was observed according to that same line of sight but at a position  $\mathbf{r} - \mathbf{v}t$  at the instant  $t = 0$ . According to the frozen turbulence hypothesis, we can then write

$$\Delta\alpha(\mathbf{r}, t) = \Delta\alpha(\mathbf{r} - \mathbf{v}t, 0). \quad (9)$$

With this translational effect, the instantaneous spatial distribution of the  $x$ -oriented mono-directional differential image motion at instant  $t$  is given by

$$\Delta\alpha(\mathbf{r}, t) = \int d\mathbf{f} |\overline{\Delta\alpha}(\mathbf{f}, 0)| \exp\{2\pi i \mathbf{f}[\mathbf{r} - \mathbf{v}t] + i\varphi_0(\mathbf{f})\}. \quad (10)$$

Relative to the observer, every spatial spectral component of frequency  $\mathbf{f}$  ‘oscillates’ at a temporal frequency  $\nu$  that is given by

$$\nu = \mathbf{f}\mathbf{v}. \quad (11)$$

With the frozen turbulence hypothesis, there is a simple relation between spatial frequencies and temporal frequencies when the velocity of the turbulent layer translation is known. The optical turbulence with a temporal frequency  $\nu$  is the result of the contributions of the optical turbulence of all the frequencies  $\mathbf{f}$  that satisfy equation (11).

Within the framework of the frozen flow hypothesis, the temporal power spectral density of the instantaneous mono-directional differential image motion  $\omega_{\Delta\alpha}^{\text{FTH}}(\nu)$  at a temporal frequency  $\nu$  is given by the sum of all the spatial power spectral densities  $W_{\Delta\alpha}(\mathbf{f})$  with frequencies  $\mathbf{f}$  that satisfy equation (11). We may symbolize this ‘energy

transfer-like’ relation by the following expression:

$$\omega_{\Delta\alpha}^{\text{FTH}}(\nu) d\nu = \int_{\nu=\mathbf{f}\mathbf{v}} d\mathbf{f} W_{\Delta\alpha}(\mathbf{f}). \quad (12)$$

In order to simplify this expression, we may choose different spatial frequency coordinates with  $\mathbf{f}' = f'_x \mathbf{i}' + f'_y \mathbf{j}'$  so that  $\mathbf{i}'$  is aligned with the direction of the velocity vector  $\mathbf{v}$ . In this case, the ‘energy transfer condition’ in equation (11) writes simply  $\nu = \mathbf{v}\mathbf{f}'$  where  $\nu$  is the module of  $\mathbf{v}$ . We can thus obtain

$$\omega_{\Delta\alpha}^{\text{FTH}}(\nu) = \frac{1}{\nu} \int d\mathbf{f}' W_{\Delta\alpha}\left(\frac{\nu}{\nu}, f'_y\right). \quad (13)$$

This is achieved by a rotation of the coordinates system. If  $\eta$  is defined by  $\mathbf{v} = \nu[\cos\{\eta\}\mathbf{i} + \sin\{\eta\}\mathbf{j}]$ , which also means that it is the angle between the velocity direction relatively to the orientation of the chosen component of the differential image motion, then we will particularly have  $f_x = f'_x \cos\{\eta\} - f'_y \sin\{\eta\}$ . This is how temporal spectra are usually calculated within the framework of the frozen turbulence hypothesis (Conan et al. 1995; Avila et al. 1997).

For example, we can consider the spatial power spectral density of the instantaneous mono-directional differential image motion as being given by

$$W_{\Delta\alpha}(\mathbf{f}) = 0.7654 \left[ \frac{C_n^2 \delta h}{\cos\{\varepsilon\}} \right] f_x^2 [f^2 + L_0^{-2}]^{-11/6} \times \left[ \frac{2J_1\{\pi Df\}}{\pi Df} \right]^2 [1 - \cos\{2\pi h \mathbf{f}\Theta\}]. \quad (14)$$

Here, diffraction and inner scale effects are neglected and the entrance pupil is circular without central obstruction.

The temporal power spectral density of the instantaneous mono-directional differential image motion in this case is thus given by

$$\omega_{\Delta\alpha}^{\text{FTH}}(\nu) = \frac{0.7654}{\nu} \left[ \frac{C_n^2 \delta h}{\cos\{\varepsilon\}} \right] \int d\mathbf{f}' \left[ \frac{\nu}{\nu} \cos\{\eta\} - f'_y \sin\{\eta\} \right]^2 \times [F^2 + L_0^{-2}]^{-11/6} \left[ \frac{2J_1\{\pi D\mathbf{f}'\}}{\pi D\mathbf{f}'} \right]^2 \times \left[ 1 - \cos \left\{ 2\pi h \Theta \left[ \frac{\nu}{\nu} \cos\{\eta - \gamma\} - f'_y \sin\{\eta - \gamma\} \right] \right\} \right], \quad (15)$$

where  $F^2 = \left[\frac{\nu}{\nu}\right]^2 + [f'_y]^2$  and  $\Theta$  being defined with  $\Theta = \Theta[\cos\{\gamma\}\mathbf{i} + \sin\{\gamma\}\mathbf{j}]$ .

The temporal power spectral density depends on the relative orientations of the wind and angular separation relatively to the chosen component of differential image motion, via the angles  $\eta$  and  $\gamma$ . Fig. 2 displays, as an example, a temporal power spectral density which is calculated by numerical integration of equation (15).

#### 5 THE OPTICAL TURBULENCE BOILING

The situation we are to describe now is the case where the turbulent layer does not translate horizontally across the observation field of view. In this case  $\mathbf{v} = 0$  explicitly. We can imagine that rather than remaining indefinitely frozen, the optical turbulence will undergo a proper evolution, the optical turbulence boiling.

In order to model this effect, we will first recall some of the earliest results of the statistical modelling of turbulence.

A fully developed and stationary turbulent fluid is statistically described with the energy cascade model. In this approach, the energy flow from large spatial structures of turbulence to smaller structures

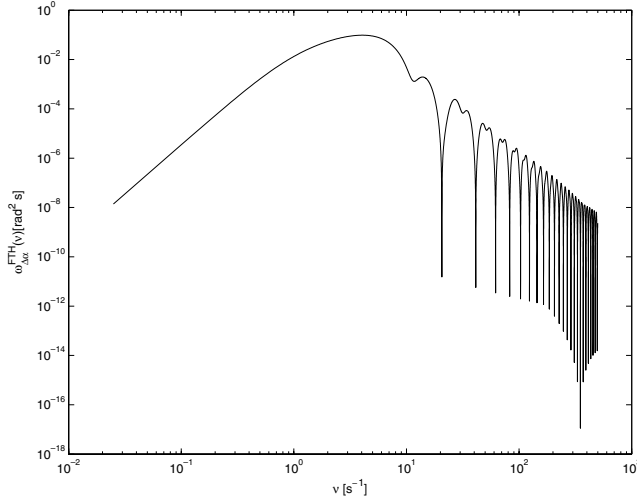


**Figure 2.** Plot of a temporal power spectral density of the instantaneous mono-directional differential image motion  $\omega_{\Delta\alpha}^{\text{FTH}}(\nu)$  within the framework of the frozen turbulence hypothesis, which is calculated by numerical integration of equation (15). Here, the term  $0.7654[\frac{C_n^2 \delta h}{\cos\{\varepsilon\}}]$  is normalized to 1.  $D = 1$  m,  $\Theta = 10$  arcsec,  $\gamma = 0$  rad,  $L_0 = 10$  m,  $h = 10$  km,  $v = 10$  m s $^{-1}$  and  $\eta = 0$  rad.

is constant. This implies through a dimensional reasoning within the framework of the Kolmogorov model that to a structure of turbulence with a given spatial characteristic length  $l$  is associated to an average velocity fluctuation  $u$  which is proportional to  $l^{1/3}$  (Tatarskii 1971).

For a turbulence structure with a spatial length  $l$ , a velocity fluctuation  $u$  is characterized by its fluctuation time  $\tau$  where  $\tau = l/u$ . This characteristic fluctuation time refers to the turbulence structure lifetime. It is an estimation of the time during which a turbulence structure appears and disappears. By replacing  $u$  by  $l^{1/3}$ , we have

$$\tau \propto l^{2/3}. \quad (16)$$

This describes how turbulence ‘boils’. The above proportionality gives a direct relation between temporal frequencies  $\nu$  and spatial frequencies  $f$  for optical turbulence. This relation is given (Masciadri & Vernin 1997; St-Jacques 1998) by

$$\nu \propto f^{2/3}. \quad (17)$$

We can introduce here a proportionality constant  $v_0$  as an independent parameter that expresses how fast the optical turbulence evolves by optical turbulence boiling. In this case, we write

$$\nu = v_0 f^{2/3}. \quad (18)$$

This also gives  $f = [\frac{\nu}{v_0}]^{3/2}$  and  $d\nu = \frac{2v_0}{3} f^{-1/3} df$ .

The spatial spectral components during the optical turbulence boiling can be viewed as resembling standing waves, each oscillating at a temporal frequency that is given by equation (18). With these considerations, the instantaneous spatial distribution of the x-oriented mono-directional differential image motion at instant  $t$  is given by

$$\Delta\alpha(\mathbf{r}, t) = \sqrt{2} \int d\mathbf{f} |\overline{\Delta\alpha}(\mathbf{f}, 0)| \cos\{2\pi v_0 f^{2/3} t + \varphi_b(\mathbf{f})\} \times \exp\{2\pi i \mathbf{f} \mathbf{r} + i\varphi_0(\mathbf{f})\}, \quad (19)$$

where  $\varphi_b(\mathbf{f})$  is an arbitrary phase with  $0 \leq \varphi_b(\mathbf{f}) < 2\pi$ . The term  $\sqrt{2} \cos\{2\pi v_0 f^{2/3} t + \varphi_b(\mathbf{f})\}$  expresses here the temporal modulation of the spatial spectral component of spatial frequency  $f$ .

Standing waves can be decomposed into two waves travelling in opposite directions.  $\Delta\alpha(\mathbf{r}, t)$  can also be rewritten in the following form:

$$\begin{aligned} \Delta\alpha(\mathbf{r}, t) = & \frac{\sqrt{2}}{2} \int d\mathbf{f} |\overline{\Delta\alpha}(\mathbf{f}, 0)| \\ & \times \exp\{2\pi i [\mathbf{f} \mathbf{r} - v_0 f^{2/3} t] + i[\varphi_0(\mathbf{f}) - \varphi_b(\mathbf{f})]\} \\ & + \frac{\sqrt{2}}{2} \int d\mathbf{f} |\overline{\Delta\alpha}(\mathbf{f}, 0)| \\ & \times \exp\{2\pi i [\mathbf{f} \mathbf{r} + v_0 f^{2/3} t] + i[\varphi_0(\mathbf{f}) + \varphi_b(\mathbf{f})]\}. \end{aligned} \quad (20)$$

Here,  $\exp\{2\pi i [\mathbf{f} \mathbf{r} - v_0 f^{2/3} t] + i[\varphi_0(\mathbf{f}) - \varphi_b(\mathbf{f})]\}$  and  $\exp\{2\pi i [\mathbf{f} \mathbf{r} + v_0 f^{2/3} t] + i[\varphi_0(\mathbf{f}) + \varphi_b(\mathbf{f})]\}$  are the expressions of the travelling waves in the spatial frequency domain whose interference produces the standing waves of the optical turbulence boiling.

We can see that every spatial frequency  $f$  leads to an equal partition of the optical turbulence energy into two temporal frequencies  $\nu = v_0 f^{2/3}$  and  $\nu = -v_0 f^{2/3}$ . As a consequence, the temporal power spectral density of the instantaneous mono-directional differential image motion  $\omega_{\Delta\alpha}^{\text{boil}}(\nu)$  is given by the following energy transfer-like expression:

$$\begin{aligned} \omega_{\Delta\alpha}^{\text{boil}}(\nu) d\nu = & \frac{1}{2} \int_{\nu=v_0 f^{2/3}} d\mathbf{f} W_{\Delta\alpha}(\mathbf{f}) \\ & + \frac{1}{2} \int_{\nu=-v_0 f^{2/3}} d\mathbf{f} W_{\Delta\alpha}(\mathbf{f}). \end{aligned} \quad (21)$$

The first integral in equation (21) deals with the positive temporal frequencies while the second integral deals with the negative ones. The temporal power spectral density is a pair function so that calculating one of the integrals is sufficient to obtain the other by symmetry. We choose to consider the positive temporal frequency part:

$$\omega_{\Delta\alpha}^{\text{boil}}(\nu; \nu > 0) d\nu = \frac{1}{2} \int_{\nu=v_0 f^{2/3}} d\mathbf{f} W_{\Delta\alpha}(\mathbf{f}). \quad (22)$$

Let us consider, for example, the simplified spatial power spectral density from equation (14). We suppose that the optical turbulence boiling relation between temporal and spatial frequencies in equation (18) is still valid beyond the inertial range even if initially derived from the Kolmogorov model.

We may reexpress this spatial power spectral density in polar coordinates  $(f, \theta_f)$  where  $f$  is the radial spatial frequency and  $\theta_f$  the polar spatial frequency. With equation (18) in mind, we can then rewrite the temporal power spectral density in the following manner:

$$\omega_{\Delta\alpha}^{\text{boil}}(\nu; \nu > 0) = \frac{3}{4v_0} \frac{\nu^2}{v_0^2} \int_0^{2\pi} d\theta_f W_{\Delta\alpha} \left( \left[ \frac{\nu}{v_0} \right]^{3/2}, \theta_f \right). \quad (23)$$

Otherwise, equation (14) becomes

$$\begin{aligned} W_{\Delta\alpha}(f, \theta_f) = & 0.7654 \left[ \frac{C_n^2 \delta h}{\cos\{\varepsilon\}} \right] [f \cos\{\theta_f\}]^2 [f^2 + L_0^{-2}]^{-11/6} \\ & \times \left[ \frac{2J_1\{\pi Df\}}{\pi Df} \right]^2 [1 - \cos\{2\pi h f \Theta \cos\{\theta_f - \gamma\}\}], \end{aligned} \quad (24)$$

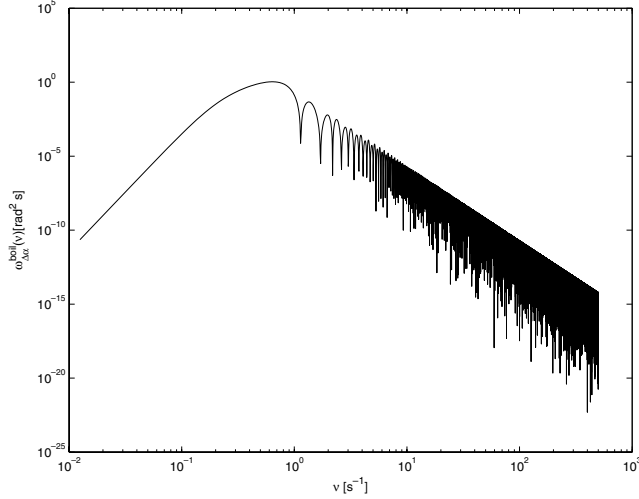


**Figure 3.** Plot of a temporal power spectral density of the instantaneous mono-directional differential image motion  $\omega_{\Delta\alpha}^{\text{boil}}(\nu)$  within the framework of the optical turbulence boiling model, which is calculated from equation (26). Here, the term  $0.7654\left[\frac{C_n^2\delta h}{\cos\{\varepsilon\}}\right]$  is normalized to 1.  $D = 1$  m,  $\Theta = 10$  arcsec,  $\gamma = 0$  rad,  $L_0 = 10$  m,  $h = 10$  km and  $\nu_0 = 1$ .

and by replacing  $W_{\Delta\alpha}(f, \theta_f)$  in equation (23) we obtain

$$\begin{aligned} \omega_{\Delta\alpha}^{\text{boil}}(\nu; \nu > 0) &= \frac{3}{4\nu_0} \left[\frac{\nu}{\nu_0}\right]^2 0.7654 \left[\frac{C_n^2\delta h}{\cos\{\varepsilon\}}\right] \left[\frac{\nu}{\nu_0}\right]^3 \\ &\times \left[ \left[\frac{\nu}{\nu_0}\right]^3 + L_0^{-2} \right]^{-11/6} \left[ \frac{2J_1\left\{\pi D \left[\frac{\nu}{\nu_0}\right]^{3/2}\right\}}{\pi D \left[\frac{\nu}{\nu_0}\right]^{3/2}} \right]^2 \\ &\times \int_0^{2\pi} d\theta_f \cos^2\{\theta_f\} [1 - \cos\{2\pi h f \Theta \cos\{\theta_f - \gamma\}\}]. \end{aligned} \quad (25)$$

The latter integral over the polar spatial frequency is easily solvable.

The positive temporal frequency part of the temporal power spectral density of the instantaneous mono-directional differential image motion in this case is then given by

$$\begin{aligned} \omega_{\Delta\alpha}^{\text{boil}}(\nu; \nu > 0) &= \frac{3\pi}{4\nu_0} 0.7654 \left[\frac{C_n^2\delta h}{\cos\{\varepsilon\}}\right] \left[\frac{\nu}{\nu_0}\right]^5 \\ &\times \left[ \left[\frac{\nu}{\nu_0}\right]^3 + L_0^{-2} \right]^{-11/6} \left[ \frac{2J_1\left\{\pi D \left[\frac{\nu}{\nu_0}\right]^{3/2}\right\}}{\pi D \left[\frac{\nu}{\nu_0}\right]^{3/2}} \right]^2 \\ &\times \left[ 1 - J_0\left\{2\pi h \Theta \left[\frac{\nu}{\nu_0}\right]^{3/2}\right\} \right] + \cos\{2\gamma\} J_2\left\{2\pi h \Theta \left[\frac{\nu}{\nu_0}\right]^{3/2}\right\}. \end{aligned} \quad (26)$$

The negative temporal frequency part of the temporal power spectral density is obtained by the same operations. The result is numerically the same.

Fig. 3 displays, as an example, a temporal power spectral density which is plotted from equation (26).

### 5.1 The optical turbulence boiling constant

It is possible to make an estimate of the numerical order of magnitude of the optical turbulence boiling constant  $\nu_0$  from experimental data. For example, a technique to test the frozen turbulence hypothesis quantitatively using data from wavefront sensors has

been developed (Schöck & Spillar 2000; St-Jacques & Baldwin 2000). In these experiments, the quantity of interest is mainly the spatio-temporal autocorrelation function of the mono-directional image motions measured through the subapertures of the wavefront sensor.

In order to interpret such results in a simple manner, we may consider distant subapertures whose relative position matches the wind direction in case of a single turbulent layer. We consider two subapertures  $a$  and  $b$  which are separated by a given distance  $L$ . The turbulence features that cross the line of sight of subaperture  $a$  reach the line of sight of subaperture  $b$  after a time interval whose duration is  $L/v$ , where  $v$  is still the velocity of the turbulent layer horizontal translation.

In the case of total validity of the frozen turbulence hypothesis, mono-directional image motion at subaperture  $b$  at instant  $t$  is exactly the same as mono-directional image motion measured at subaperture  $a$  at instant  $t - L/v$ . This means that the spatio-temporal covariance of mono-directional image motion at distance  $L$  and time interval  $L/v$  is given by the variance of mono-directional image motion anywhere. Now if during its travel from subaperture  $a$  to subaperture  $b$  turbulence undergoes proper evolution, then the spatio-temporal covariance of mono-directional image motion at distance  $L$  and time interval  $L/v$  is given by the temporal covariance of mono-directional image motion at time interval  $L/v$ , where only the optical turbulence boiling is involved.

It appears that the time interval for which the temporal covariance (of the mono-directional image motion variance) reaches half its maximum is typically of the order of 50 to 100 ms for most available data sets (Schöck & Spillar 2000). With this, we can evaluate the typical values of the optical turbulence boiling constant.

Following the same operations as for the mono-directional differential image motion in Section 5, the simplified temporal power spectral density of the instantaneous mono-directional image motion measured through circular subapertures when only the optical turbulence boiling occurs is given by

$$\begin{aligned} \omega_{\alpha}^{\text{boil}}(\nu; \nu > 0) &= \frac{3\pi}{4\nu_0} 0.3827 \left[\frac{C_n^2\delta h}{\cos\{\varepsilon\}}\right] \left[\frac{\nu}{\nu_0}\right]^5 \\ &\times \left[ \left[\frac{\nu}{\nu_0}\right]^3 + L_0^{-2} \right]^{-11/6} \left[ \frac{2J_1\left\{\pi D \left[\frac{\nu}{\nu_0}\right]^{3/2}\right\}}{\pi D \left[\frac{\nu}{\nu_0}\right]^{3/2}} \right]^2. \end{aligned} \quad (27)$$

The temporal covariance  $R_{\alpha}(\tau)$  for a time interval  $\tau$  relates to it by

$$R_{\alpha}(\tau) = 2 \int_0^{\infty} d\nu \omega_{\alpha}^{\text{boil}}(\nu; \nu > 0) \cos\{2\pi\nu\tau\}. \quad (28)$$

For various values of  $\nu_0$ , we can calculate the time interval  $t_{50}$  (Schöck & Spillar 2000) for which  $R_{\alpha}(t_{50}) = \frac{1}{2}R_{\alpha}(0)$  with the previous equations. We then find an approximate relationship between the experimental results  $t_{50}$  and the possibly related optical turbulence boiling constant  $\nu_0$  in the following simple form:

$$\nu_0 \approx [9.84t_{50}]^{-1}. \quad (29)$$

We have assumed the near-field approximation for the optical turbulence by neglecting diffraction and scintillation and we have assumed an arbitrary value  $L_0 = 10$  m for the outer scale as a plausible order of magnitude. The diameter of the subapertures is  $D = 10$  cm.

$t_{50}$  varies between 50 and 100 ms in the data we have considered. The optical turbulence boiling constant  $\nu_0$  then varies between approximately 2 and 1. This gives us an order of magnitude for  $\nu_0$

even if we have not yet enough data for the amplitude of variations of this parameter.

## 6 THE TRANSLATING-AND-BOILING OPTICAL TURBULENCE MODEL

In the most general case, turbulence layer boils while translating horizontally above the observer. We propose in the following a theoretical approach to model the optical turbulence temporal evolution when the optical turbulence boiling and the turbulence layer horizontal translation above the observer are simultaneously involved.

We recall that  $\Delta\alpha(\mathbf{r}, t)$  is an instantaneous spatial distribution of the x-oriented mono-directional differential image motion as measured through a ground-based telescope. At a given initial instant  $t = 0$ , it is given by equation (8).

As stated before, each spectral component with spatial frequency  $f$  oscillates at a temporal frequency  $\nu_0 f^{2/3}$ . Simultaneously, the same spatial spectral components of the optical turbulence translate at a velocity  $v$ .

By applying the same modelling of the horizontal translation as in equation (10) and the same modelling of the optical turbulence boiling as in equation (19), the instantaneous spatial distribution of the x-oriented mono-directional differential image motion at instant  $t$  can be expressed as

$$\Delta\alpha(\mathbf{r}, t) = \sqrt{2} \int d\mathbf{f} |\overline{\Delta\alpha}(\mathbf{f}, 0)| \cos \{2\pi\nu_0 f^{2/3} t + \varphi_b(\mathbf{f})\} \times \exp\{2\pi i \mathbf{f}[\mathbf{r} - \mathbf{v}t] + i\varphi_0(\mathbf{f})\}, \quad (30)$$

where  $\varphi_0(\mathbf{f})$  and  $\varphi_b(\mathbf{f})$  are arbitrary phases.

For the observer, the temporal behaviour of a given spatial spectral component is thus that of an oscillation at a given temporal frequency which is modulated by an oscillation at another temporal frequency.

We can rewrite  $\Delta\alpha(\mathbf{r}, t)$  from equation (30) into the following form:

$$\Delta\alpha(\mathbf{r}, t) = \frac{\sqrt{2}}{2} \int d\mathbf{f} |\overline{\Delta\alpha}(\mathbf{f}, 0)| \times \exp \{2\pi i [\mathbf{f}\mathbf{r} - [\mathbf{f}\mathbf{v} + \nu_0 f^{2/3}]t] + i[\varphi_0(\mathbf{f}) - \varphi_b(\mathbf{f})]\} + \frac{\sqrt{2}}{2} \int d\mathbf{f} |\overline{\Delta\alpha}(\mathbf{f}, 0)| \times \exp \{2\pi i [\mathbf{f}\mathbf{r} - [\mathbf{f}\mathbf{v} - \nu_0 f^{2/3}]t] + i[\varphi_0(\mathbf{f}) + \varphi_b(\mathbf{f})]\}. \quad (31)$$

We can see here that every spatial frequency  $f$  leads to an equal partition of the optical turbulence energy into two temporal frequencies  $\nu = \mathbf{f}\mathbf{v} + \nu_0 f^{2/3}$  and  $\nu = \mathbf{f}\mathbf{v} - \nu_0 f^{2/3}$ .

Consequently, the temporal power spectral density  $\omega_{\Delta\alpha}(\nu)$  of the x-oriented differential image motion is given by the following energy transfer expression:

$$\omega_{\Delta\alpha}(\nu)d\nu = \frac{1}{2} \int_{\nu=\mathbf{f}\mathbf{v}+\nu_0 f^{2/3}} d\mathbf{f} W_{\Delta\alpha}(\mathbf{f}) + \frac{1}{2} \int_{\nu=\mathbf{f}\mathbf{v}-\nu_0 f^{2/3}} d\mathbf{f} W_{\Delta\alpha}(\mathbf{f}). \quad (32)$$

Resolving this equation is not as straightforward as it is when dealing with boiling or horizontal translation effects separately. We did not find an analytic solution to equation (32), so we treated it numerically. There are two complementary approaches to take benefit from this model. One may need for instance to numerically simulate a time series of instantaneous measurements. We present

in Section 6.1 a method for numerically simulating the optical turbulence temporal evolution as presented in this section and in the previous one. Section 6.2 presents a numerical procedure to obtain a good estimation of the temporal power spectral densities of the instantaneous x-oriented mono-directional differential image motion and other optical turbulence quantities.

### 6.1 Monte Carlo numerical simulation of the optical turbulence boiling

The above analytical modelling has a direct applicability. It provides a simple way to simulate the temporal evolution of spatial (or angular) distributions of optical turbulence observable quantities through the field of view of a telescope. When applied to phase and amplitude fluctuations, it can have a direct relevance for adaptive optics studies for example (Vogel 2006). We introduce in the following the general principles of a simulation of differential image motion while keeping in mind that the procedure is exactly the same for phase, amplitude or differential piston fluctuations to give a few examples.

A spatial two-dimensional distribution of differential image motion at an arbitrary instant  $t = 0$  is given by equation (8). Such a spatial distribution  $\Delta\alpha(\mathbf{r}, 0)$  is usually obtained numerically over a regularly sampled grid by putting

$$\Delta\alpha(\mathbf{r}, 0) = \text{FFT}^{-1} \{ \sqrt{W_{\Delta\alpha}(\mathbf{f})} [A_1(\mathbf{f}) \cos\{\varphi_0(\mathbf{f})\} + iA_2(\mathbf{f}) \sin\{\varphi_0(\mathbf{f})\}] \}, \quad (33)$$

where FFT denotes the Fast Fourier Transform procedure,  $A_1(\mathbf{f})$  and  $A_2(\mathbf{f})$  are independent Gaussian random numbers with variance equal to 1 and  $\varphi_0(\mathbf{f})$  are independent random numbers with uniform distribution and satisfying  $0 < \varphi_0(\mathbf{f}) \leq 2\pi$  as we have seen before. The spatial distribution  $\Delta\alpha(\mathbf{r}, 0)$  is random but it is ensured that its statistical properties are reproducible through  $W_{\Delta\alpha}(\mathbf{f})$ .

Within the framework of the Frozen Turbulence Hypothesis, if we take a particular measurement at a given position at an initial instant, measurements at other moments are simply obtained from the positions on the same spatial distribution according to equation (9). The entire spatial distribution is moved in front of the observer.

In the model of the optical turbulence boiling, every spatial spectral component of frequency  $f$  ‘oscillates’ at a given temporal frequency  $\nu$  according to equation (18).

Equation (19) illustrates how the spatial components ‘oscillate’ over time and consequently how the spatial distribution of differential image motion ‘boils’. We have thus a spatial spectrum at every instant  $t$  and this makes it possible to obtain numerically the spatial distribution at any moment by performing the following transform:

$$\Delta\alpha(\mathbf{r}, t) = \sqrt{2} \text{FFT}^{-1} \{ \sqrt{W_{\Delta\alpha}(\mathbf{f})} \cos \{2\pi\nu_0 f^{2/3} t + \varphi_b(\mathbf{f})\} \times [A_1(\mathbf{f}) \cos\{\varphi_0(\mathbf{f})\} + iA_2(\mathbf{f}) \sin\{\varphi_0(\mathbf{f})\}] \} \quad (34)$$

where  $\varphi_b(\mathbf{f})$  are independent random numbers with uniform distribution that satisfy  $0 \leq \varphi_b(\mathbf{f}) < 2\pi$ . Its randomness, which is attributed to the spatial spectral component, ensures that the temporal evolution is random and unpredictable while its statistical properties are reproducible through  $W_{\Delta\alpha}(\mathbf{f})$  and through how energy is distributed over temporal frequencies.

The result of such a simulation can be viewed as a three-dimensional grid with one of its axis being time. It is then possible, by taking measurements at different spatial positions on layers corresponding to different instants, to have the temporal evolution of differential image motion including the optical turbulence boiling and horizontal translation.

The numerical simulation principle is briefly introduced here and more details will probably be discussed in a forthcoming paper.

## 6.2 Numerical estimation of temporal spectra

In both the cases of the frozen turbulence hypothesis and of the optical turbulence boiling without horizontal translation, solving the equations of energy transfer from spatial to temporal frequencies (equations 12 and 21) has been analytically straightforward. It consisted schematically in fixing a value to the temporal frequency  $\nu$  and to look for all the possible values of the spatial frequencies  $f$  that satisfy the relations between  $\nu$  and  $f$ , given by equations (11) and (18). For every fixed temporal frequency, the corresponding spatial frequencies provide an integration domain which is simple in shape for both the cases previously referred to.

When considering the translating and boiling optical turbulence, the spatial frequency integration domains for fixed temporal frequencies are far more complex and we find it difficult to apply the same analytical reasoning as above to calculate temporal power spectral densities through several scans.

The simplest way to numerically solve equation (32) is to scan all the spatial frequencies and to assign their optical turbulence energy to the corresponding temporal frequencies. We have chosen to perform a semirandom sampling of spatial frequencies so that we ensure a better coverage of the optical turbulence spatial power spectral densities through several scans.

Temporal frequencies are regularly sampled with a sampling path  $\delta\nu$ . Meanwhile, the spatial frequency domain is mapped with square cells with dimensions  $\delta f \times \delta f$  within which  $f$  are randomly sampled. To each spatial frequency  $f$  is associated the corresponding optical turbulence energy  $W_{\Delta\alpha}(f)$ . Otherwise, two temporal frequencies  $\nu = f\nu + \nu_0 f^{2/3}$  and  $\nu = f\nu - \nu_0 f^{2/3}$  are also associated with  $f$ . The procedure consists of then adding the amount of energy  $\frac{1}{2} \frac{\delta f^2}{\delta\nu} W_{\Delta\alpha}(f)$  to the temporal power spectral density  $\omega_{\Delta\alpha}(\nu)$  at the corresponding temporal frequencies  $\nu$ . At the end of the scan, the optical turbulence energy in  $W_{\Delta\alpha}(f)$  is redistributed over  $\omega_{\Delta\alpha}(\nu)$  with respect to the relation between spatial and temporal frequencies. This is a very schematic description of the principle of the numerical procedure and does not include, for example, the improvement which consists of an adaptive mapping of the spatial frequency domain for an optimized sampling of the lower frequencies.

In practice, because the temporal frequency sampling path  $\delta\nu$  is nonzero, the numerical procedure does not give the temporal power spectral density  $\omega_{\Delta\alpha}(\nu)$  exactly but an average over  $\delta\nu$ . In fact, the result can be formally expressed by a convolution product  $\omega_{\Delta\alpha}(\nu) \otimes \pi\{\nu/\delta\nu\}$  where  $\pi\{\nu/\delta\nu\}$  is the rectangle function of base  $\delta\nu$ . A special care must then be taken for temporal frequency samplings and for temporal covariance calculations. The procedure has been implemented and successfully tested on the already known cases of the frozen turbulence hypothesis and the optical turbulence boiling without horizontal translation. The temporal power spectra are exactly the same in both the cases as those obtained analytically.

The resulting temporal power spectral densities from numerical calculations are as expected different in shape from the temporal power spectral densities obtained when the optical turbulence boiling or horizontal translation is ignored. Fig. 4 displays, as an example, a temporal power spectral density that has been calculated numerically from equation (32). It can be visually compared to Fig. 2 where  $\nu_0$  is put equal to zero and to Fig. 3 where  $\nu$  is put equal to zero.

## 7 EFFECT OF THE OPTICAL TURBULENCE BOILING ON DIFFERENTIAL IMAGE MOTION

When a temporal spectrum  $\omega_{\Delta\alpha}(\nu)$  is calculated for a given set of parameters, it is then possible to calculate the temporal covari-

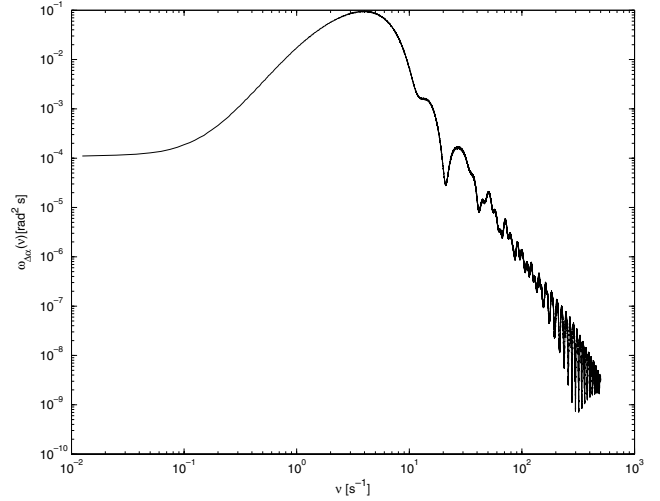


**Figure 4.** Plot of a temporal power spectral density of the instantaneous mono-directional differential image motion  $\omega_{\Delta\alpha}(\nu)$  when both the optical turbulence boiling and the horizontal translation are involved. Here, the term  $0.7654 \left[ \frac{C_0^2 \delta h}{\cos[\epsilon]} \right]$  is normalized to 1.  $D = 1$  m,  $L_0 = 10$  m,  $h = 10$  km,  $\Theta = 10$  arcsec,  $\gamma = 0$  rad,  $\nu = 10$  m s $^{-1}$ ,  $\eta = 0$  rad and  $\nu_0 = 1$ .

ance of the instantaneous mono-directional differential image motion  $R_{\Delta\alpha}(\tau)$  with equation (5), and then to calculate the statistical variance of the finite-exposure mono-directional differential image motion  $\sigma_T^2$  with equation (4). This latter depends upon the shape of the temporal covariance, and so upon how fast the optical turbulence becomes uncorrelated.

Let us consider a situation where the optical turbulence is well described except for the optical turbulence boiling contribution. One can therefore calculate the variance of the finite-exposure one-directional differential image motion in the framework of the frozen flow hypothesis, thus assuming  $\nu_0 = 0$ , as a predictive characterization of the accuracy of astrometrical measurements for example. With the model we propose in the previous sections, we can introduce the optical turbulence boiling as a perturbation to the frozen flow hypothesis conditions in order to observe the difference.

The introduction of the optical turbulence boiling should reduce the coherence time that is due to the translating effect. It is then tempting to consider the optical turbulence boiling as being beneficial for differential astrometry because when the differential image motion is decorrelated faster, it means a decrease of the variance of finite-exposure differential image motion, as well as the astrometric error. It would be damaging at the same time for adaptive optics since it would mean that the optical turbulence evolves faster.

We can see, however, that in some conditions, introducing the optical turbulence boiling may increase the variance of finite-exposure differential image motion. Fig. 5, for example, displays the variance  $\sigma_T^2$  as a function of exposure time  $T$  in case of some values of the optical turbulence boiling constant  $\nu_0$ . One may note that in this particular configuration where the wind is parallel to the spatial projection of the angular separation, the variance  $\sigma_T^2$  increases instead of decreasing.

It may be surprising at a first sight that a more uncorrelated optical turbulence would lead to an increase of the finite-exposure variance. This is understandable when considering the shape of the temporal covariance of the instantaneous one-directional differential image motion in this configuration where the wind is parallel to the angular separation spatial projection. In Fig. 6, one can see

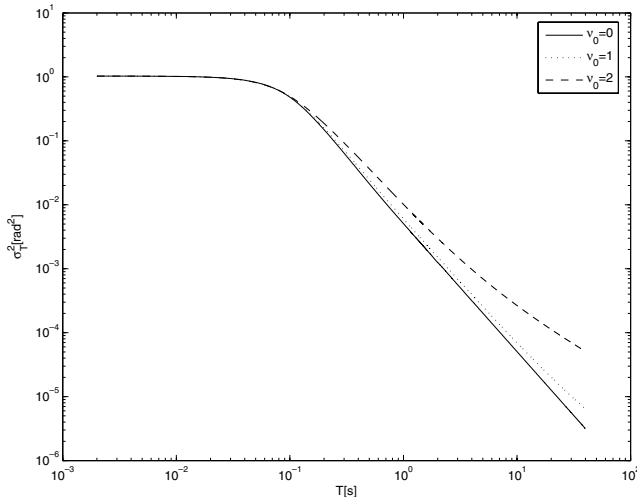


**Figure 5.** Plot of the statistical variance of the finite-exposure mono-directional differential image motion  $\sigma_T^2$  as a function of exposure time  $T$  for some fixed values of the optical turbulence boiling constant  $\nu_0$ . Here, the term  $0.7654[\frac{C_n^2 \delta h}{\cos[\varepsilon]}]$  is normalized to 1.  $D = 1$  m,  $L_0 = 10$  m,  $h = 10$  km,  $\Theta = 10$  arcsec,  $\gamma = 0$  rad,  $v = 10$  m s $^{-1}$  and  $\eta = 0$  rad.

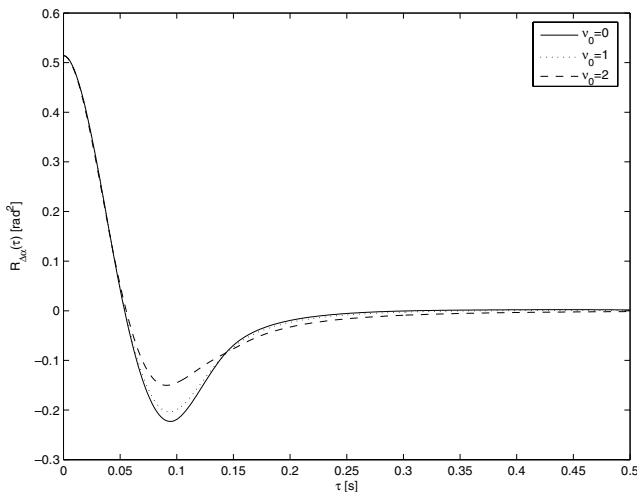


**Figure 6.** Plot of the temporal covariance of the instantaneous mono-directional differential image motion  $R_{\Delta\alpha}(\tau)$  for some fixed values of the optical turbulence boiling constant  $\nu_0$ . Here, the term  $0.7654[\frac{C_n^2 \delta h}{\cos[\varepsilon]}]$  is normalized to 1.  $D = 1$  m,  $L_0 = 10$  m,  $h = 10$  km,  $\Theta = 10$  arcsec,  $\gamma = 0$  rad,  $v = 10$  m s $^{-1}$  and  $\eta = 0$  rad.

that the covariance in the case of the frozen turbulence hypothesis ( $\nu_0 = 0$ ) has positive and negative values on different domains of the temporal separation  $\tau$ . The negative part corresponds mainly to large temporal separations over which the instantaneous mono-directional differential image motion has a statistical tendency to be in opposite directions. Equation (4) otherwise shows that the variance of finite-exposure fluctuations is a weighted integral of the temporal covariance of the instantaneous fluctuations. When the optical turbulence boiling is introduced, it mainly affects those parts of the temporal covariance that correspond to the larger temporal separations. This leads to a rapid disappearance of the negative covariance zones so that the variance increases rapidly. Fig. 6 shows how the temporal covariance of the instantaneous one-directional

differential image motion can be affected by a relatively slow optical turbulence boiling. It can be observed that even in the presence of strong winds, the contribution of the optical turbulence boiling may be very notable, especially for long exposures.

What appears is that a precise determination of the variance of finite-exposure differential image motion requires the determination of the optical turbulence boiling constant  $\nu_0$  alongside with the other parameters such as the wind velocity and its orientation according to the angular separation.

It also appears from this application to mono-directional differential image motion that the optical turbulence boiling is a significant contributor to the description of the accuracy of ground-based differential astrometry through the optical turbulence and that it deserves to be properly investigated in order to perform astrometric measurements in the most suitable conditions.

## 8 CONCLUSION

We have proposed over this contribution a theoretical modelling of the optical turbulence temporal evolution, which is based upon some phenomenological assumptions and which is applied here to finite-exposure differential image motion. We have shown how it is possible to calculate temporal spectra of the optical turbulence quantities in the general case in which both the turbulent layer horizontal translation and the optical turbulence boiling are involved. The model is quantitatively expressed within the framework of a one-layer turbulence configuration with the von Kármán optical turbulence model. It can be easily generalizable into multilayered configurations and using other optical turbulence models.

The major aim of this contribution is to propose a theoretical approach to model the optical turbulence temporal evolution and its effects on modelling finite-exposure differential image motion when the turbulent layer horizontal translation and the optical turbulence boiling are both involved. We have also discussed the possible implications of such a model on ground-based differential astrometry. The calculations, however, have to be pursued more systematically in order to completely characterize the most favourable conditions for astrometric measurements. The implications of such a modelling of the optical turbulence temporal evolution have also to be investigated in other areas of the high angular resolution and confronted with experimental data.

## REFERENCES

- Aime C., Kadiri S., Ricort G., 1980, *Opt. Commun.*, 35, 169
- Aime C., Borgnino J., Martin F., Petrov R., Ricort G., Kadiri S., 1986, *J. Opt. Soc. Am.*, 3, 1001
- Anderson J., Bedin L. R., Piotto G., Yadav R. S., Bellini A., 2006, *A&A*, 454, 1029
- Avila R., Ziad A., Borgnino J., Matin F., Agabi K., Tokovinin A., 1997, *J. Opt. Soc. Am.*, 14, 3070
- Berdja A., Borgnino J., Irbah A., 2006, *J. Opt. A: Pure Appl. Opt.*, 8, 244
- Borgnino J., 1990, *Appl. Opt.*, 29, 1863
- Borgnino J., Martin F., Ziad A., 1992, *Opt. Commun.*, 91, 267
- Casertano S., Lattanzi M. G., Perryman M. A. C., Spagna A., 1996, *Ap&SS*, 241, 89
- Chauvin G., Lagrange A.-M., Dumas C., Zuckerman B., Mouillet D., Song I., Beuzit J.-L., Lowrance P., 2005, *A&A*, 438, L25
- Conan J.-M., Rousset G., Madaec P.-Y., 1995, *J. Opt. Soc. Am.*, 12, 1559
- Davis J., North J. R., 2001, *Publ. Astron. Soc. Aust.*, 18, 281
- Fitzgerald M. P., Graham J. R., 2006, *ApJ*, 637, 541
- Gatewood G. D., 1987, *ApJ*, 94, 213
- Gendron E., Léna P., 1996, *Ap&SS*, 239, 221

- Gubler J., Tytler D., 1998, *PASP*, 110, 738  
Innocenti C., Consortini A., 2004, *Proc. SPIE*, 5237, 25  
Jolissaint L., Véran J.-P., Conan R., 2006, *J. Opt. Soc. Am.*, 23, 382  
Kellerer A., Tokovinin A., 2007, *A&A*, 461, 775  
Lane F., Muterspaugh M. W., 2004, *ApJ*, 601, 1129  
Lattanzi M. G., Spagna A., Sozzetti A., Casertano S., 2000, *MNRAS*, 317, 211  
Launhardt R., 2005, *Astron. Nachr*, 326, 563  
Lazorenko P. F., 2006, *A&A*, 449, 1271  
Lazorenko P. F., Lazorenko G. A., 2004, *A&A*, 427, 1127  
Lindegren L., 1980, *A&A*, 89, 41  
Lopez B., 1992, *A&A*, 253, 635  
Lopez B., Sarazin M., 1993, *A&A*, 276, 320  
Masciadri E., Vernin J., 1997, *Appl. Opt.*, 36, 1320  
McAlister H. A., 1996, *Ap&SS*, 241, 77  
Pravdo S. H., Shaklan S. B., 1996, *ApJ*, 465, 264  
Roddier F., Gilli J. M., Lund G., 1982, *J. Optics (Paris)*, 13, 263  
Roddier F., Northcott M. J., Graves J. E., McKenna D. L., Roddier D., 1993, *J. Opt. Soc. Am.*, 10, 957  
Schöck M., Spillar E. J., 1999, *Proc. SPIE*, 3762, 225  
Schöck M., Spillar E. J., 2000, *J. Opt. Soc. Am.*, 17, 1650  
Shao M., Colavita M. M., 1992, *A&A*, 262, 353  
Sozzetti A., 2005, *PASP*, 117, 1021  
Sozzetti A., Casertano S., Brown R. A., Lattanzi M. G., 2003, *PASP*, 115, 1072  
St-Jacques D., 1998, PhD thesis, Univ. Cambridge  
St-Jacques D., Baldwin J. E., 2000, *Proc. SPIE*, 4006, 951  
Tatarskii V. I., 1971, *The Effects of the Turbulent Atmosphere on Wave Propagation*. Israel Program for Scientific Translations, Jerusalem  
Vernin J., Roddier F., 1973, *J. Opt. Soc. Am.*, 63, 270  
Vernin J., Weigelt G., Caccia J.-L., Müller M., 1991, *A&A*, 243, 553  
Vogel C. R., 2006, *Proc. SPIE*, 6272, 627229

This paper has been typeset from a  $\text{\TeX}/\text{\LaTeX}$  file prepared by the author.